Rapid Re-Design and Bandwidth/Size Trade-Offs for Compact Wideband Circular Polarization Antennas Using Inverse Surrogates and Fast EM-Based Parameter Tuning

Ubaid Ullah, Slawomir Koziel, *Senior Member*, *IEEE,* and Ismail Ben Mabrouk

Abstract—**Design of compact wideband circularly polarized (CP) antennas is challenging due to the necessity of simultaneous handling of several characteristics (reflection, axial ratio, gain) while maintaining a small size of the structure. Antenna re-design for various operating bands is clearly more difficult yet practically important because intentional reduction of the bandwidth (e.g., by moving the lower edge of the operating band up in frequency) may lead to a considerable size reduction, which can be beneficial for specific application areas. This paper proposes a rigorous approach to rapid re-design of miniaturized CP antennas involving inverse surrogate models and fast electromagnetic (EM)-based parameter tuning. Our methodology allows for a precise control of the lower operating frequency of the CP antenna (both in terms of the impedance and axial ratio bandwidth) and accomplishing the geometry parameter scaling at an extremely low cost of a few EM analyses of the structure at hand. Our methodology is demonstrated by re-designing a compact wide slot CP antenna in the range of 3.2 GHz to 5.8 GHz. The proposed approach can be used for fast rendering of the bandwidth/size trade-offs (the footprints obtained for the verification structure range from 783 mm^2 to 482mm^2), thus determining the most suitable designs for particular applications. The numerical findings are validated experimentally.**

Index Terms—**Circular polarization antennas, wideband antennas, surrogate modeling, rapid re-design, simulation-driven design, inverse modeling.**

I. INTRODUCTION

WIDEBAND operation and circular polarization (CP) are highly desirable features of antennas for modern wireless communication due to high data capacity and high-resolution requirements. Wideband antennas are important for accommodating ever-increasing demands for system functionality, whereas CP is essential to ensure reliable data transmission [1-3]. Some of the many practical benefits of circularly polarized antennas include mitigation of the signal interference, reduction of multi-path losses and polarization mismatch, as well as alleviation of the Faraday's effects [4]. In the process of advancing wireless technology, considerable research efforts have been directed towards the development of various types of circularly polarized antennas. These include dielectric resonator antennas [5], printed monopoles and dipoles [6-8], as well as the most common class of microstrip patch antennas (MPAs) [9-10]. MPAs generally require a large ground plane, which limits both their impedance and the CP bandwidth. In order to meet the increasing bandwidth requirements, a considerable number of topologies have been proposed for planarly-structured CP antennas with the emphasis on wide-slot antennas. The advantage of this particular type of antenna is geometrical flexibility and convenient excitation [11-12]. Moreover, due to a low quality factor, these antennas are inherently wideband. This has been demonstrated by many researchers for both linearly polarized and CP structures [13-17].

The aforementioned shape flexibility of wide-slot antennas becomes the major source of their design challenges. Both the electrical and field properties of the antenna (including circular polarization) depend on the slot shape, which, in principle, can be arbitrary. Consequently, the conventional way of designing wide-slot antennas involves experience-driven heuristic approaches based on the simulated field distribution on the surface of the structure at any given stage of the antenna topology development. The process is necessarily based on repetitive (thus expensive) full-wave electromagnetic (EM) analyses as any theoretical predictions of the operating frequency for arbitrary-shaped slotsare extremely complicated if not impossible. To alleviate these difficulties, the characteristics mode analysis has been implemented to obtain a physical understanding of generic wide-slot antennas [18-21]. However, this information is only limited to the particular shape that has been analyzed and cannot be generalized and applied to other shapes which therefore require individual analysis. Furthermore, the characteristic mode technique is independent of the source type and position and only depends on the shape and the size of the conducting object. Therefore, the predictions based on

U.Ullah and Ismail Mabrouk are with Networks and Communication Engineering department, Al Ain university of Science and Technology, P.O.Box (112612), Abu Dhabi, UAE. (ubaid.ullah@aau.ac.ae, ismail.mabrouk@aau.ac.ae). S. Koziel is with Engineering Optimization and Modeling Center of Reykjavik University, Reykjavik, Iceland and also withthe Faculty of Electronics, Telecommunications and Informatics, Gdansk University of Technology, 80-233 Gdansk, Poland (e-mail: koziel@ru.is)

this technique may vary from the actual response of the externally fed antennas.

The literature indicates that a large number of different slot shapes can be used to realize wideband CP antennas. These include basic shapes such as circular or rectangular, as well as irregular shapes [22-27]. Due to geometrical complexity and the lack of complete information about the behavior of these structures, it is difficult to predict their characteristics and re-design them for other operating frequencies. Vast majority of the reported structures [11-17] are case studies concerned with particular applications and presenting wideband CP antenna operating at, and optimized for particular frequency ranges. No indicationsare typically given on how to scale the antenna geometry for other frequencies. Clearly, the development of a simple and computationally efficient re-design methodology would be indispensable to extend applicability of the reported structures.

This paper proposes a rigorous approach to rapid re-design of wideband circularly polarized antennas. Our approach capitalizes on the recently proposed inverse surrogate modeling technique for a fast geometry scaling of high-frequency structures [28], which is supplemented here with a forward design correction stage involving a fast electromagnetic (EM)-based parameter tuning. The proposed methodology allows for a precise control of the lower operating frequency of the CP antenna (both in terms of the impedance and the axial ratio bandwidth) and accomplishing the geometry parameter scaling at an extremely low cost of a few EM analyses of the structure at hand. The major contributions of the paper include: (i) development of a complete framework for low-cost wideband CP antenna re-design; (ii) adaptation of the inverse surrogate modeling approach [28] and development of EM-based forward correction; (iii) demonstration (both numerical and experimental) of successful CP antenna geometry scaling with respect to the operating frequency as well as good control of both reflection and axial ratio in-band levels; (iv) practical (e.g., incurring low CPU cost) generation of a set of bandwidth-size trade-off designs. None of these has been previously reported in the literature.

Validation of the method has been carried out by re-designing a compact wide-slot CP antenna—in terms of its lower operating frequency—in the range of 3.2 GHz to 5.8 GHz. As demonstrated, the re-design process can be accomplished at the cost of a few (three to five) EM simulations of the antenna, while controlling the operating frequency with a good precision and ensuring satisfactory reflection and axial ratio levels within the entire operating band. Our technique can be used for rapid generation of the bandwidth/size trade-offs (the footprints obtained for the verification structure range from 783 mm^2 to 482 mm^2), thus determining the most suitable designs for particular applications. Experimental validation of the selected design is also provided.

II. CASE STUDY

The purpose of this section is to introduce a particular geometry of a wideband wide-slot CP antenna to be used as a case study throughout the work. Using this exemplary structure, the challenges pertinent to the CP antenna re-design will be demonstrated. More importantly, the structure will illustrate the re-design procedure proposed in Section III.

The antenna [29] is implemented on Rogers RO4003C substrate ($\varepsilon_r = 3.38$, $\tan\delta = 0.0027$, $h = 0.813$ mm). The front and the back view of the structure has been shown in Fig. 1. The antenna feeding network involves a metal-backed CPW and an inverted L-shape parasitic strip placed in a close proximity to the microstrip line extension of the length L_m. The coplanar spacing g between the ground planes and microstrip line feed is fixed at 50-ohm. The fundamental requirements for CP is excitation of two simultaneous electric field components with equal amplitudes and 90-degree phase shift. The orthogonal (horizontal/vertical) electric field components (here, denoted as E_x and E_y) are attributed to the high impedance parasitic strips placed along the x-axis and the y-axis, respectively.

To facilitate the design process, it is imperative to handle a possibly small number of variables. Consequently, the parameters that are not effecting the CP and impedance bandwidth are kept fixed. The coplanar spacing g=0.6325 mm,$g_1 = 0.48$ mm and $g_2 = 0.33$ mm, the widths of the parasitic strips $W_v = 1.37$ and W_h= 2.16, and microstrip line monopole W_m= 1.35mm are dimensioned at the initial design stage and subsequently fixed. A modified geometry of the wide rectangular slot shown in Fig. 1(b) is etched in the backside ground plane. The parameters (W_c, L_c, W_{s1}, L_{s1}, L_{s2},W_{s2}) defining the dimensions of the slots controls the width of the edges on the back side of the antenna. The additional current paths created on the circumference of the wide-slot adds to the enhancement of the CP bandwidth. This particular design has been optimized at a full-wave level of description and characterized for S_{11} and AR at 4.2 GHz. More details concerning the antenna operating principles and performance can be found in [29].

The traditional way of designing a wide-slot type antenna involves a tedious heuristic approach, which leads to the stage-by-stage development of the antenna structure. The final topology is then optimized for a certain frequency band, usually using expensive parameter sweeping, often combined with other (more rigorous) optimization methods. The design obtained this way is operating at a particular frequency band, which is typically quite poorly controlled by the designer. For example, many designs reported in the literature feature excessively wide impedance bandwidth as compared to the axial-ratio bandwidth [2], [3]. Additionally, wide-slot CP antennas are very sensitive to some of their parameters, i.e., even slight parameter alterations lead to considerable degradation of the impedance matching the AR. Clearly, under these circumstances, re-design of the CP antenna for different frequency ranges becomes a major undertaking.
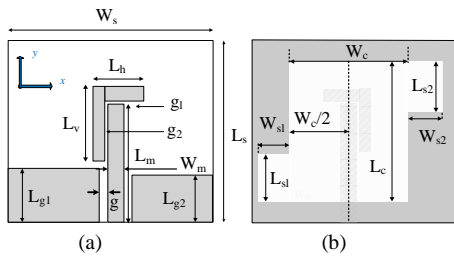
Fig. 1. Configuration of the parameterized reference antenna; metallization marked using gray color: (a) front view (b) back view.

Such a re-design is of otherwise considerable practical value because maintaining the operating band (especially its lower end) as required by a particular application allows us, among others, to reduce the structure physical dimensions as much as possible (again, assuming a particular operating band).

For the sake of illustration, a simple engineering insight-driven re-design procedure of the antenna of Fig. 1, initially optimized for 4.2 GHz is discussed. In order to lower the operating frequency of the antenna, the current path on the periphery of the slot is lengthened by incrementing all the dimensions with the same ratio. As can it be observed from the antenna responses shown in Fig.2, increasing the dimensions of the antenna results in lowering the AR operating frequency to approximately 3.7 GHz but with almost 70-percent degradation in the AR. Similarly, when the dimensions are decreased, the operating frequency is shifted upward to 4.5 GHz but the acceptance criteria ($S_{11} \leq -10$ dB and $AR \leq 3$ dB) are largely violated. In order to bring the characteristics to satisfactory levels, antenna dimensions need to be re-optimized which is—from the computational perspective—the task as challenging as obtaining the initial (or reference) design.

### III. CP ANTENNA DESIGN TRADE-OFFS AND GEOMETRY SCALING METHODOLOGY

In this section, the framework for computationally efficient re-design of CP antennas with respect to the operating frequency range is formulated. Verification cases will be discussed in Section IV.

A. Problem Formulation. CP Antenna Design Trade-Offs

Although wideband CP antennas are typically designed to extend the impedance matching and axial ratio bandwidth [14], [15], precise adjustment of the lower edge of the operating range f_L allows us to control the antenna size which primarily depends on f_L. As explained in the introduction, this parameter is rarely "designed" but it is typically a by-product of a particular antenna topology and the ability of the designer to boost the performance parameters (including the bandwidth) using a combination of experience, parameter sweeping, and numerical optimization. Here, we are interested in rendering designs that feature precisely adjusted operating frequency ranges. This permits, among others, yielding geometries that constitute the trade-offs between the antenna bandwidth and its physical dimensions.
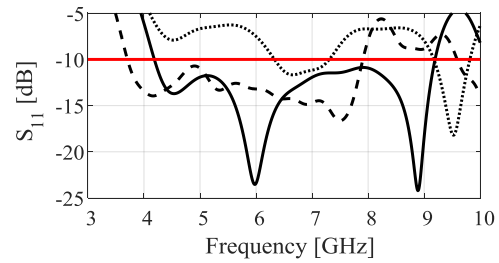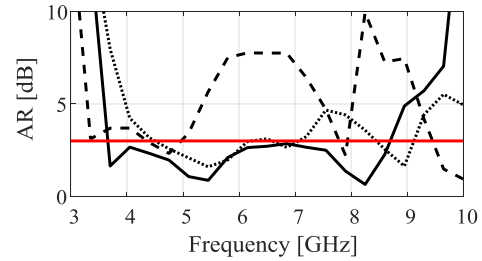
Fig. 2. Antenna responses at different designs: the reference design (lower edge of the operating bandwidth equal to 4.2 GHz) (—),antenna initially re-designed for 3.7GHz (- - -), antenna initially re-designed for 4.5 GHz (····): (a) S_{11} (b) AR.

For the purpose of our considerations, $x \in R^n$ will represent the vector of antenna geometry parameters, whereas $S(x)$ and $AR(x)$ will stand for the EM-simulated reflection and axial ratio characteristics. Although other antenna responses (e.g., the gain) can also be included in the design process, the proposed methodology will be explained and demonstrated using these two performance figures, which already poses considerable practical challenges as indicated in Section II. We will also denote by $x(f_L)$ the design that is optimized to satisfy the following requirements:

- Reflection $S(x(f_L)) \leq -10$ dB for the frequencies $f \geq f_L$;
- Axial ratio $AR(x(f_L)) \leq 3$ dB for the frequencies $f \geq f_L$.

Additionally, a certain maximum frequency f_H is selected up to which both conditions should hold. More specifically, although the antenna re-design will be realized with respect to f_L, the assumption is that the antenna bandwidth extends to the common f_H for the entire range of $f_{L.\min} \leq f_L \leq f_{L.\max}$ considered.

B. Geometry Scaling Using Inverse Surrogates

The initial re-design is realized using the methodology adopted from [28]. In the first step, several reference designs $x(f_{L.k})$ are pre-optimized to satisfy the conditions of Section II.A for the frequencies $f_{L.k}$, $k = 1, ..., N$, allocated within the range of interest from $f_{L.\min}$ to $f_{L.\max}$. These designs can be already available (e.g., from the previous design work with the same antenna structures) or obtained specifically for the re-design purposes.

The second step is the construction of an inverse surrogate model $s(f_L)$ by approximating the reference designs $x(f_{L.k})$. It is referred to as "inverse" because its input argument is the intended frequency f_L, whereas the output is the vector of antenna geometry parameters corresponding to f_L. The model

components are denoted as $x_{s.k}(f_L, \boldsymbol{p}_k)$, $k = 1, \ldots, n$ (n is the number of antenna parameters), in which $\boldsymbol{p}_k$ stand for the coefficients to be identified. Thus, we have

$$s(f_L, \boldsymbol{P}) = \left[x_{s.1}(f_L, \boldsymbol{p}_1) \; \ldots \; x_{s.n}(f_L, \boldsymbol{p}_n) \right]^T \tag{1}$$

The overall parameter vector $\boldsymbol{P} = [\boldsymbol{p}_1 \; \ldots \boldsymbol{p}_n]$. Similarly, as in [28], the following analytical form of the surrogate is assumed:

$$x_{s.k}(f_L) = p_1 + p_2 \cdot \exp(p_3 f_L) \tag{2}$$

where $\boldsymbol{p} = [p_1 p_2 p_3]$. An exponential function has been found to provide a reasonable representation of the relationship between the operating frequencies and geometry parameter values for antennas [30]. Also, the number of model coefficients should be small in order to be able to identify the major trends using a small number of reference designs without making the underlying regression problem underdetermined.

Surrogate model identification is realized through the least-square regression

$$\boldsymbol{p}_k = \arg \min_{\boldsymbol{p}} \sum_{j=1}^{N} (x_{s.k}(f_{L.j}, \boldsymbol{p}) - x_{j.k})^2, \quad k = 1, \ldots, n \tag{3}$$

where $x_{j.k}$ is the kth component of $\boldsymbol{x}(f_{L.j})$.

Assuming that the surrogate adequately represents the manifold containing the optimum designs $\boldsymbol{x}(f_L)$ within the range of interest, the surrogate does return the optimum design for any given $f_L \in [f_{L.\min} f_{L.\max}]$. In other words, we have $\boldsymbol{x}(f_L) \approx s(f_L, \boldsymbol{P})$.

Unfortunately, it is not possible to obtain a perfect representation of the aforementioned manifold using a limited number of reference designs. Consequently, a correction is necessary. In this work, it is realized in two steps. Assuming that the actual lower operating frequency of the antenna obtained as $\boldsymbol{x}(f_L)$ is $f_L + df_L$ (with df_L being a re-design error), the first correction step is accomplished by re-evaluating the inverse model as follows

$$\boldsymbol{x}(f_L) = s(f_L - df_L, \boldsymbol{P}) \tag{4}$$

The correction (4) handles, to a certain extent, the geometry parameter scaling inaccuracies concerning the operating frequencies. The second correction stage is described in Section II.C. Note that the cost of (4) is only a single EM simulation of the antenna (necessary to verify df_L).

C. Warm Start Forward Correction Using Trust-Region Gradient Search with Broyden Updates

The major issue with the antenna re-design using the inverse surrogate of Section II.B is that the relevant characteristics, here, the reflection and the axial ratio are not directly controlled in the process. Consequently, upon executing (4), the antenna responses may violate the conditions $S(\boldsymbol{x}(f_L)) \leq -10$ dB, $AR(\boldsymbol{x}(f_L)) \leq 3$ dB, and still be slightly misaligned with respect to f_L. All of these are fixed in the second correction stage which is essentially a trust-region (TR) gradient search [31]. In each iteration, the algorithm updates the design as

$$\boldsymbol{x}(f_L) \leftarrow \arg \min_{\boldsymbol{x}; \, -\boldsymbol{d} \leq \boldsymbol{x} - \boldsymbol{x}(f_L) \leq \boldsymbol{d}} U(\boldsymbol{L}_S(\boldsymbol{x}), \boldsymbol{L}_{AR}(\boldsymbol{x})) \tag{5}$$

where

$$\boldsymbol{L}_S(\boldsymbol{x}) = S(\boldsymbol{x}(f_L)) + \boldsymbol{J}_S(\boldsymbol{x}(f_L)) \cdot (\boldsymbol{x} - \boldsymbol{x}(f_L)) \tag{6}$$

$$\boldsymbol{L}_{AR}(\boldsymbol{x}) = AR(\boldsymbol{x}(f_L)) + \boldsymbol{J}_{AR}(\boldsymbol{x}(f_L)) \cdot (\boldsymbol{x} - \boldsymbol{x}(f_L)) \tag{7}$$

are the linear expansion models of S and AR, respectively, with $\boldsymbol{J}_S$ and $\boldsymbol{J}_{AR}$ being their Jacobians. The meaning of (5) is that the linear models, representing the antenna responses (reflection and axial ratio characteristics) are optimized within the interval $[\boldsymbol{x} - \boldsymbol{d}, \boldsymbol{x} + \boldsymbol{d}]$ to yield a candidate design $\boldsymbol{x}_{tmp}$, which is accepted if $U(S(\boldsymbol{x}_{tmp}), AR(\boldsymbol{x}_{tmp})) < U(S(\boldsymbol{x}(f_L)), AR(\boldsymbol{x}(f_L)))$, i.e., the (EM-simulated) objective function value at the candidate design is better than at the previous design $\boldsymbol{x}(f_L)$ (in which cases we assign $\boldsymbol{x}(f_L) = \boldsymbol{x}_{tmp}$). Otherwise, $\boldsymbol{x}_{tmp}$ is rejected and the optimization process is restarted with the reduced TR size $\boldsymbol{d}$. The TR size vector $\boldsymbol{d}$ is adjusted using the standard rules [31], based on the gain ratio ρ defined as

$$\rho = \frac{U(S(\boldsymbol{x}_{tmp}), AR(\boldsymbol{x}_{tmp})) - U(S(\boldsymbol{x}(f_L)), AR(\boldsymbol{x}(f_L)))}{U(\boldsymbol{L}_S(\boldsymbol{x}_{tmp}), \boldsymbol{L}_{AR}(\boldsymbol{x}_{tmp})) - U(\boldsymbol{L}_S(\boldsymbol{x}(f_L)), \boldsymbol{L}_{AR}(\boldsymbol{x}(f_L)))} \tag{8}$$

which is the ratio of the actual (EM-simulated) versus linear-model-predicted objective function improvement. In particular, we have $\boldsymbol{d} \leftarrow 2\boldsymbol{d}$ if $\rho > 0.75$, and $\boldsymbol{d} \leftarrow \boldsymbol{d}/3$ if $\rho < 0.25$. The sub-problem (5) is solved using Matlab's *fmincon* routine which is a general purpose algorithm for continuous constrains optimization based on the sequential quadratic programming procedure.

The objective function is defined as

$$U(S, AR) = [AR(\boldsymbol{x}, f_L) - 3]^2 + \beta_1 d_S(\boldsymbol{x})^2 + \beta_2 d_{AR}(\boldsymbol{x})^2 \tag{9}$$

in which

$$d_S(\boldsymbol{x}) = \max\{\max\{f_L \leq f \leq f_H : S(\boldsymbol{x}, f) + 10\}, 0\} \tag{10}$$

$$d_{AR}(\boldsymbol{x}) = \max\{\max\{f_L \leq f \leq f_H : AR(\boldsymbol{x}, f) - 3\}, 0\} \tag{11}$$

Here, the explicit dependence of S and AR on frequency has been marked; f_H is the maximum frequency of interest (user-defined, cf. Section III.A). The penalty terms d_S and d_{AR} quantify a possible violation of the requirements $S(\boldsymbol{x}(f_L)) \leq -10$ dB, $AR(\boldsymbol{x}(f_L)) \leq 3$ dB within the frequency range of interest, whereas the primary objective is defined to ensure that the actual AR bandwidth starts at f_L; β_k, $k = 1, 2$, are the penalty coefficients.

Normally, the TR algorithm evaluates the Jacobians using finite differentiation which makes the process CPU intensive, especially for highly-dimensional parameter spaces [32]. In this work, in order to maintain computational efficiency, the two mechanisms are incorporated into the process:

1. The Jacobians are initialized using the sensitivity data from one of the reference designs (the one that realized $\min\{k : |f_{L.k} - f_L|\}$). These Jacobians are already available from the optimization process of the reference points;

2. For subsequent iterations, a rank-one Broyden update [33] is used instead of finite differentiation. More specifically, we have:

$$\boldsymbol{J}_S \leftarrow \boldsymbol{J}_S + \frac{(\boldsymbol{f} - \boldsymbol{J}_S \cdot \boldsymbol{h}) \cdot \boldsymbol{h}^T}{\boldsymbol{h}^T \boldsymbol{h}} \tag{12}$$

in which $\boldsymbol{f} = S(\boldsymbol{x}(f_L)) - S(\boldsymbol{x}(f_L)^{old})$, and $\boldsymbol{h} = \boldsymbol{x}(f_L) - \boldsymbol{x}(f_L)^{old}$ (the superscript *old* stands for the parameter vector before the update (5)).

The above mechanisms reduce the cost of the correction (5) to a single EM simulation of the antenna per iteration, and are justified because the required design adjustment is typically minor as it will be demonstrated in Section IV.

D. Redesign Procedure

The entire re-design procedure is summarized here. Figure 3(a) shows the flow diagram of constructing the inverse surrogate model, whereas Fig. 3(b) explains the re-design process itself. Note that surrogate construction is a separate routine because, once the model is ready, it can be reused multiple times to re-design the antenna for various operating frequencies.

IV. NUMERICAL RESULTS AND EXPERIMENTAL VALIDATION

The procedure of Section III is demonstrated here for the antenna of Fig. 1 (cf. Section II). The objective is to re-design the structure for the selected lower operating frequencies f_L within the range 3.2 GHz to 5.8 GHz. Three reference designs have been pre-optimized for the purpose of inverse surrogate model construction. We have $\boldsymbol{x}(f_{L.1})$ = [7.73 7.27 6.24 8.34 16.27 22.0 13.06 8.27 10.36 5.96 16.19 16.19 8.38 22.8]^T, $\boldsymbol{x}(f_{L.2})$ = [6.91 5.93 4.65 8.93 15.74 21.95 11.78 7.59 9.72 5.76 12.79 12.79 8.37 22.5]^T, and $\boldsymbol{x}(f_{L.3})$ = [5.29 5.10 1.50 12.11 14.61 20.56 12.98 5.23 9.72 5.08 10.5 10.5 8.99 21.0]^T. Their characteristics have been shown in Fig. 4. The average simulation time of the antenna is 2.5 minutes, whereas the average cost of finding the reference design is 180 EM antenna simulations, which is the major contributor to surrogate model construction. Note that the axial ratio upper frequency for the 3.2 GHz design is slightly below 8 GHz, therefore, the maximum frequency of interest f_{max} has been set up to 8 GHz (cf. Section III.*C*, below (9)). Figure 5 shows the extracted inverse surrogate model for the selected antenna parameters. Note that the model is interpolative because the number of reference designs coincides with the number of model coefficients.
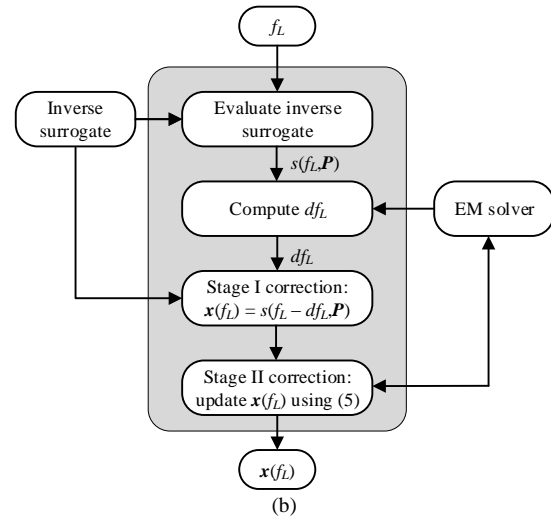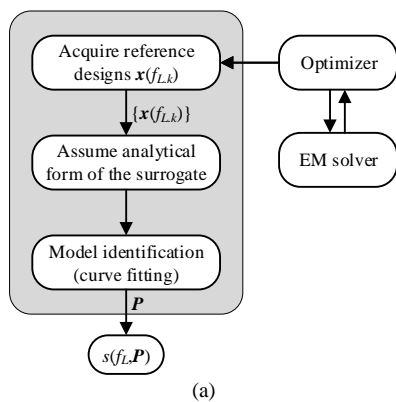

(a)

(b)

Fig. 3. Flow diagram of surrogate-assisted CP antenna re-design procedure: (a) inverse model construction, (b) re-design process.

For the sake of verification, the antenna of Section II has been re-designed for the following five lower operating frequencies: 3.5 GHz, 3.8 GHz, 4.5 GHz, 5.0 GHz, and 5.5 GHz. Table I shows the geometry parameter values of the antenna upon applying the procedure of Section III, whereas Fig. 6 shows the reflection and axial ratio characteristics. It can be observed that the inverse surrogate already provides a decent design, especially for the first three verification frequencies. For the remaining two cases, a certain amount of overshoot can be noticed.

As demonstrated in Section II, the antenna characteristics are very sensitive to some of the parameters so that the designs obtained from the surrogate can be considered satisfactory.

The first correction stage considerably improves the antenna characteristics in terms of providing a better alignment with the required values of f_L. The second stage essentially realizes fine-tuning. The final designs indicate that the proposed approach does ensure a precise control over the lower operating frequency.

At the same time, the reflection and axial ratio levels are maintained below −10 dB and 3 dB, respectively. It should be emphasized that our methodology is computationally efficient. The overall cost of accomplishing the re-design process is only between three to five EM simulations of the antenna structure, which is between 10 to 15 minutes of the CPU time.

The verification designs gathered in Table I also illustrate possible trade-offs between the antenna bandwidth and its physical dimensions. The footprint ranges from 742 mm^2 to 535 mm^2 (or from 783 mm^2 to 482 mm^2 if the reference designs are included). This means that the proposed methodology allows us to yield the antenna design that features the minimum possible footprint for a particular lower operating frequency. Consequently, it can be considered a useful tool in making educated design decisions in the context of specific applications.
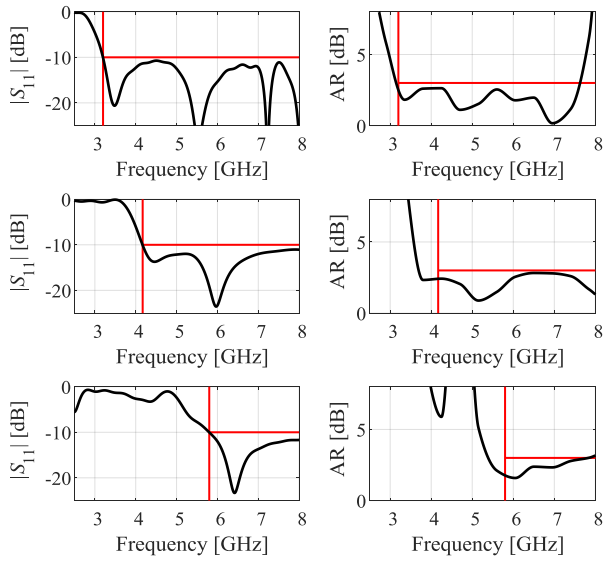
Fig. 4. Reflection and axial ratio characteristics for the three reference designs, corresponding to the lower operating frequencies of 3.2 GHz (top), 4.17 GHz (middle), and 5.8 GHz (bottom). The vertical lines represent the mentioned frequencies, whereas the horizontal lines mark the −10 dB and 3 dB acceptance levels for $|S_{11}|$ and AR, respectively.
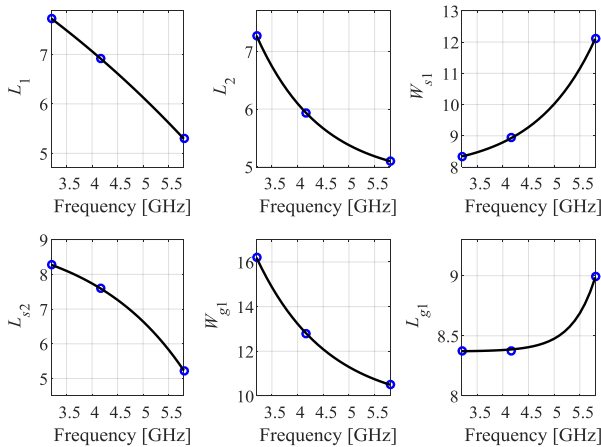

Fig. 5. Inverse surrogate for the CP antenna of Section II for selected geometry parameters: geometry parameter values at the reference designs (o), and the inverse model (—).

An important comment should be made at this point, which is that the presented re-design procedure is not oriented towards size reduction but towards obtaining the design that has a particular lower operating frequency (and maintains acceptable reflection and minimum AR within its operating band). Therefore, is it possible to further reduce the antenna size by explicit (EM-driven) footprint minimization. In such a process, the antenna footprint becomes the primary objective, whereas the acceptance thresholds for the reflection and AR within the operating band are enforced by constraints similar to those discussed in Section III.*C*. For the sake of illustration, the 5.5 GHz design has been re-optimized for minimum size yielding the footprint of 400 mm² with the outer dimensions of $L_s = 21.5$ mm and $W_s = 18.6$ mm. Clearly, this incurs additional computational expenses.
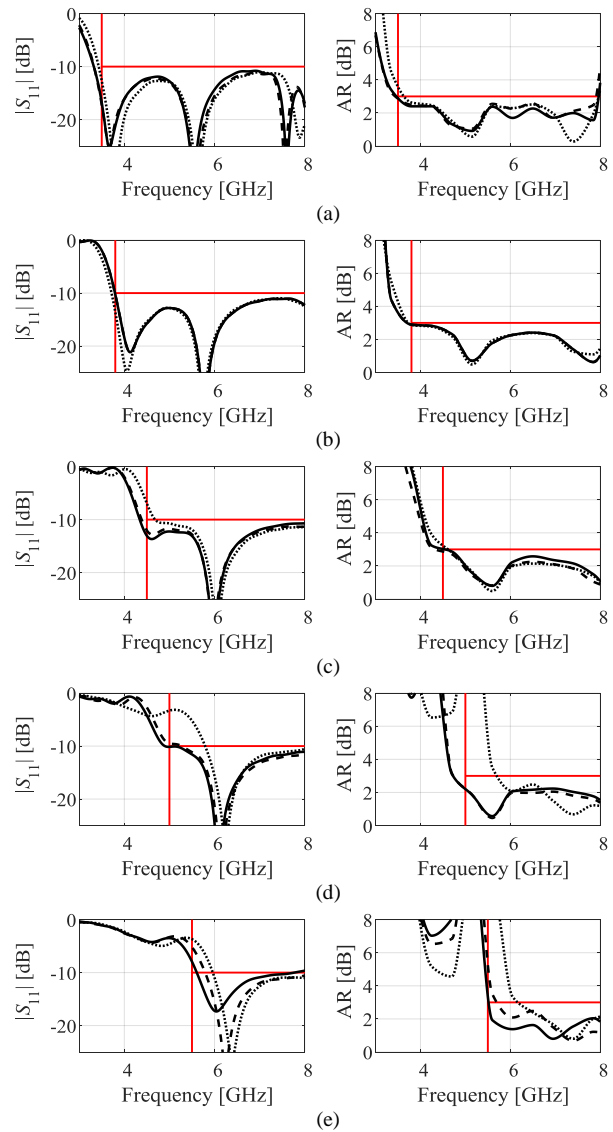

Fig. 6. Reflection and axial ratio characteristics for the antenna of Section II redesigned for five lower operating frequencies of (a) 3.5 GHz, (b) 3.8 GHz, (c) 4.5 GHz, (d) 5.0 GHz, and (e) 5.5 GHz (bottom). The vertical lines represent the mentioned frequencies, whereas the horizontal lines mark the −10 dB and 3 dB acceptance levels for $|S_{11}|$ and AR, respectively. Design obtained directly from the inverse surrogate (····), design upon the first stage of correction (- - -), and final design obtained after the second correction stage (—).

Two of the verification designs, namely the 3.5 GHz and 5.0 GHz ones have been fabricated and measured for additional validation. Figure 7 shows the photographs of the fabricated prototypes. The simulated and measured S_{11}, AR and realized gain of the two fabricated designs are illustrated in Fig. 8. Vertical lines mark the intended lower operating frequencies of the antenna. It can be clearly observed from the reflection and AR responses that both the antennas maintain wideband characteristics with excellent agreement between simulation and measurements. The average realized gain of the antennas within the CP operating bandwidth is 3.47 dBic with the peak gain of 4dBi. The simulated and measured radiation patterns in the *xz*-plane and the *yz*-plane are depicted in Figs. 9 and 10, respectively. A stable bi-directional radiation characteristic in both planes can be observed at all the frequency points in the ±*z*-direction.

V.   BENCHMARKING

The antenna operating at the lowest operating frequency is compared with the recent state-of-the-art designs in terms of AR, S_{11}, and size of the antenna. As indicated in Table II, the proposed antenna outperforms the reference designs in all of the performance figures.

TABLE I GEOMETRY PARAMETERS OF RE-DESIGNED CP ANTENNA

| Geometry parameters	Lower operating frequency f_L				
	3.5 GHz	3.8 GHz	4.5 GHz	5.0 GHz	5.5 GHz
L_v	7.51	7.17	6.53	6.33	6.65
L_h	6.93	6.23	5.80	5.59	5.43
L_{s1}	6.29	5.16	4.39	3.88	3.18
W_{s1}	8.66	8.70	9.07	9.40	10.07
L_m	16.17	15.86	15.55	15.40	15.09
L_c	22.04	21.80	21.54	21.37	21.09
W_c	12.57	12.60	12.61	12.62	12.71
L_{s2}	7.76	7.65	7.11	6.77	6.30
W_{s2}	10.05	9.87	10.24	9.72	9.74
L_{g2}	5.93	5.78	5.62	5.53	5.44
W_{g1}	15.32	13.58	12.46	11.90	8.65
W_{g2}	15.32	13.58	12.46	11.90	8.65
L_{g1}	8.36	8.38	8.42	8.49	8.60
L_s	22.69	22.46	22.15	21.94	21.71
W_s	32.62	29.14	26.90	25.78	24.65
Antenna footprint [mm^2]	740.14	654.48	595.89	565.66	535.42

(a)

(b)
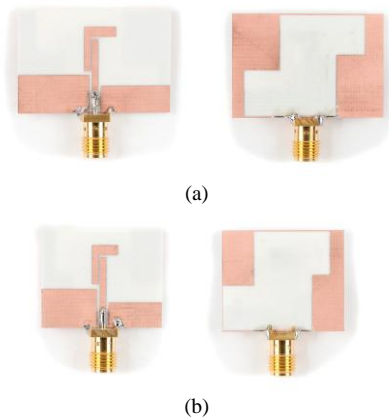
Fig. 7. Photographs of the fabricated verification designs: (a) design for f_L = 3.5 GHz, (b) design for f_L = 5.0 GHz. Front (left) and back (right).
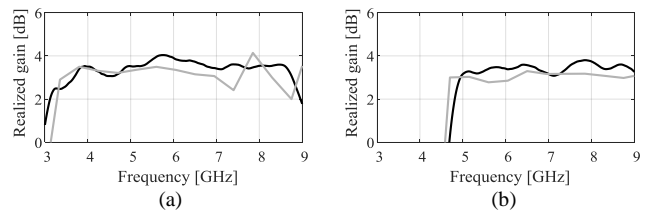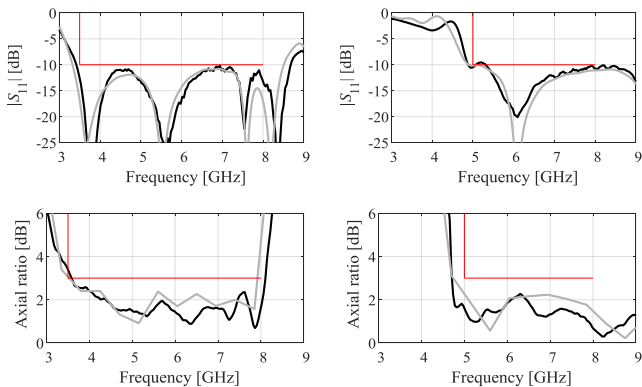

Fig. 8. Reflection, axial ratio, and realized gain characteristics: (a) design for f_L = 3.5 GHz, (b) design for f_L = 5.0 GHz. Simulation (gray) and measurement (black). Vertical lines mark the intended lower operating frequency, horizontal lines mark the acceptance levels for $|S_{11}|$ and AR.

TABLE II COMPARISON WITH STATE-OF-THE-ART CP ANTENNAS

Ref	%AR	%BW	Size [λ_o^2]	Substrate (h (mm), ε)
[4]	42	42.6	0.17	RT(0.81, 3.38)
[17]	49	62	0.20	AD(0.762, 2.5)
[34]	27	50.2	0.23	FR4 (1.6,4.4)
[35]	41.3	84	0.28	RT(1.6, 2.2)
[36]	27.45	71.63	0.42	FR4 (1.6,4.4)
[37]	39.4	57	0.78	AD(0.762, 2.5)
[38]	40	90.2	0.28	FR4 (1.6,4.4)
[39]	27	111	0.38	FR4 (0.8, 4.4)
[40]	14	27	0.13	FR4 (0.8, 4.4)
[41]	22	37	0.89	RT(0.8, 4.4)
[42]	42	55.5	0.15	FR4 (1,4.4)
Proposed	81	89	0.09	RT(0.81, 3.38)

It should be emphasized that the purpose of the paper is a presentation of the rapid re-design procedure, which is the novelty of the work, rather than a presentation of the particular antenna topology, which was merely selected as a demonstration example.
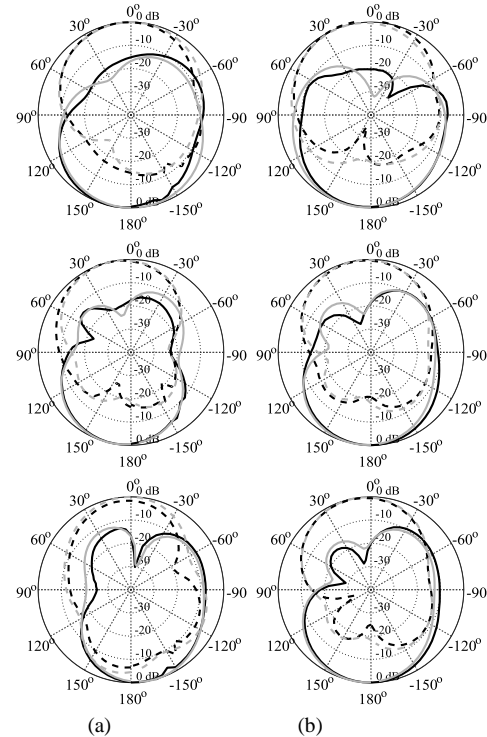

(a)   (b)

Fig. 9.   Simulated (gray) and measured (black) radiation pattern of the proposed antenna in the xz-plane with RHCP (solid) and LHCP (dashed): (a) design for f_L = 3.5 GHz (patterns shown at frequencies, from top to bottom: 3.5 GHz, 5.5 GHz, 7.5 GHz), (b) design for f_L = 5.0 GHz (patterns shown at frequencies, from top to bottom: 5.5 GHz, 6.5 GHz, 7.5 GHz).
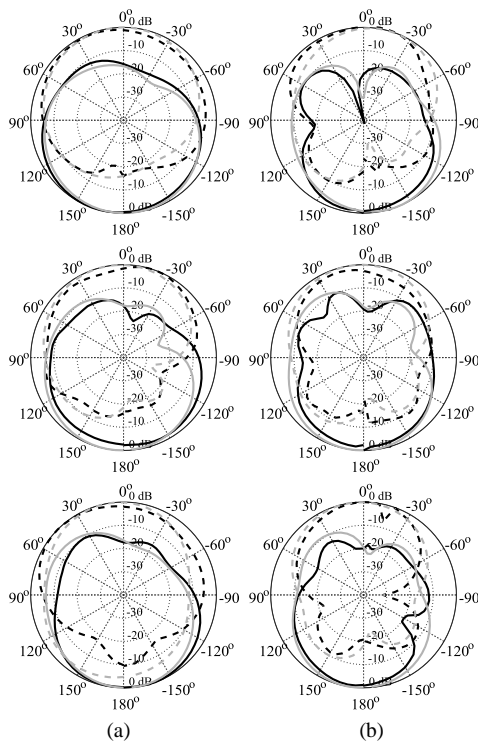
Fig. 10. Simulated (gray) and measured (black) radiation pattern of the proposed antenna in the *yz*-plane with RHCP (solid) and LHCP (dashed): (a) design for f_L = 3.5 GHz (patterns shown at frequencies, from top to bottom: 3.5 GHz, 5.5 GHz, 7.5 GHz), (b) design for f_L = 5.0 GHz (patterns shown at frequencies, from top to bottom: 5.5 GHz, 6.5 GHz, 7.5 GHz).

VI. CONCLUSION

In this paper, a rigorous and computationally efficient approach for re-design of miniaturized CP antennas has been proposed. Our methodology involves inverse surrogate models and fast EM-based parameter tuning. A combination of inverse-model-based geometry scaling and forward correction of antenna characteristics allows for precise control of the operating band and, consequently, yielding the designs that feature possibly small sizes (given particular lower operating frequencies of choice). The proposed technique has been demonstrated using a particular example of a wide-slot CP antenna. Our numerical and experimental results indicate that rapid re-design can be realizedwithin a wide range of operating frequencies, here,from 3.2 GHz to 5.8 GHz. At the same time, both the reflection and the axial ratio responses are kept within the acceptable levels throughout the operating band. Furthermore, the computational cost of the re-design process is kept extremely low (a few EM analyses of the structure at hand). The presented method can be used to fast rendering of the bandwidth/size trade-offs and, consequently, determining the most suitable designs for the intended applications. The future work will include the extension of the method to allow handling other antenna characteristics such as gain, as well as to permit explicit size reduction of the structure at hand.

ACKNOWLEDGMENT

REFERENCES

[1] M. Aziz ulHaq, S. Koziel, and Q. S. Cheng, "EM-driven size reduction of UWB antennas with ground plane modifications," *2017 International Applied Computational Electromagnetics Society Symposium (ACES)*, Suzhou, pp. 1-2, 2017.

[2] R. Xu, J. Li, and W. Kun, "A broadband circularly polarized crossed-dipole antenna," *IEEE Trans. Antennas Propag*., vol. 64, no. 10, pp. 4509-4513, Oct. 2016.

[3] M. Nosrati and N. Tavassolian, "Miniaturized circularly polarized square slot antenna with enhanced axial-ratio bandwidth using an antipodal Y strip," *IEEE Antennas Wireless Propag. Lett.,* vol. 16, pp. 817-820, 2017.

[4] U. Ullah and S. Koziel, "Design and optimization of a novel miniaturized low-profile circularly polarized wide-slot antenna" *Journal of Electromagnetic Waves and Applications*., vol. 32, pp. 2099-2109, 2018.

[5] M. F. Ain, U. Ullah, and Z.A. Ahmad. "Bi-Polarized dual-segment rectangular dielectric resonator antenna," *IETE Journal of Res.*, vol.59, pp.739–743, 2013.

[6] T. Fujimoto, T. Ishikubo, and M. Takamura, "A wideband printed elliptical monopole antenna for circular polarization,"*IEICE Trans. Commun.,* vol. E100-B, no. 2, pp. 203–210, Feb. 2017.

[7] K. Ding, C. Gao, Y. Wu, D. Qu, and B. Zhang, "A broadband circularly polarized printed monopole antenna with parasitic strips,"*IEEE Antennas Wireless Propag. Lett.,*vol. 16, pp. 2509–2512, 2017.

[8] H. Tang, K. Wang, R. Wu, C. Yu, J. Zhang, and X. Wang, "A novel broadband circularly polarized monopole antenna based on C-shaped radiator,"*IEEE Antennas Wireless Propag. Lett.,* vol. 16, pp. 964–967, 2017.

[9] C. Sun, H. L. Zheng, L. F. Zhang, and Y. Liu, "Analysis and design of a novel coupled shorting strip for compact patch antenna with bandwidth enhancement," *IEEE Antennas Wireless Propag. Lett*., vol. 13, pp. 1477– 1481, 2014.

[10] R. Xu, J.-Y. Li, K. Wei, and G.-W. Yang, "Broadband rotational symmetry circularly polarized antenna,"*Electron. Lett.,* vol. 52, no. 6, pp. 414–416, Mar. 2016.

[11] J. Wei, X. Jiang, and L. Peng, "Ultrawideband and high-gain circularly polarized antenna with double-Y-shape slot,"*IEEE Antennas Wireless Propag. Lett.,* vol. 16, pp. 1508–1511, 2017.

[12] K. Ding, C. Gao, T. Yu, D. Qu, and B. Zhang, "Gain-improved broadband circularly polarized antenna array with parasitic patches,"*IEEE Antennas Wireless Propag. Lett.,*vol. 16, pp. 1468–1471, 2016.

[13] M. S. Ellis, Z. Zhao, J. Wu, X. Ding, Z. Nie, and Q.-H. Liu, "A novel simple and compact microstrip-fed circularly polarized wide slot antenna with wide axial ratio bandwidth for C-band applications," *IEEE Trans. Antennas Propag.,* vol. 64, no. 4, pp. 1552–1555, Apr. 2016.

[14] K. O. Gyasi, G. Wen, D. Inserra, Y. Huang, J. Li, A.E. Ampoma, and H. Zhang,"A compact broadband cross-shaped circularly polarized planar monopole antenna with a ground plane extension," *IEEE Antennas Wireless Propag. Lett.,*vol. 17, no. 2, pp. 335–338, Feb. 2018.

[15] R. Xu, J.-Y. Li, J.-J. Yang, K. Wei, and Y.-X. Qi,"A design of U-shaped slot antenna with broadband dual circularly polarized radiation,"*IEEE Trans. Antennas Propag.,* vol. 65, no. 6, pp. 3217–3220, Jun. 2017.

[16] T. T. Le, H. H. Tran, and H. C. Park, "Simple-structured dual-slot broadband circularly polarized antenna,"*IEEE Antennas Wireless Propag. Lett.,*vol. 17, no. 3, pp. 476–479, Mar. 2018.

[17] U. Ullah and S. Koziel, "A broadband circularly polarized wide-slot antenna with a miniaturized footprint," *IEEE Antennas and Wireless Propagation Lett*, vol. 17, no. 12, pp. 2454-2458, Dec. 2018.

[18] M. Khan and D. Chatterjee, "Characteristic mode analysis of a class of empirical design techniques for probe-fed, U-slot microstrip patch antennas," *IEEE Trans. Antennas Propag.,* vol. 64, no. 7, pp. 2758–2770, Jul. 2016.

[19] E. Antonino-Daviu, M. Cabedo-Fabrés, M. Sonkki, N. M. Mohamed-Hicho, and M. Ferrando-Bataller, "Design guidelines for the excitation of characteristic modes in slotted planar structures,"*IEEE Trans. Antennas Propag.,* vol. 64, no. 12, pp. 5020–5029, Dec. 2016.

[20] J. Zhao, Y. Chen, and S. Yang, ''In-band radar cross-section reduction of slot antenna using characteristic modes,'' *IEEE Antennas Wireless Propag. Lett.,*vol. 17, no. 7, pp. 1166–1170, Jul. 2018.

[21] J. K. Pakkathillam and M. Kanagasabai, "Circularly polarized broadband antenna deploying fractal slot geometry,"*IEEE Antennas Wireless Propag. Lett.,*vol. 14, pp. 1286–1289, 2015.

[22] K. Saraswat and A. R. Harish,"Analysis of wideband circularly polarized ring slot antenna using characteristics mode for bandwidth enhancement,"*Int. J. RF. Microw. Comput. Aided Eng.,* vol. 28, no. 2, p. e21186, Feb. 2018.

[23] H. H. Tran, N. Nguyen-Trong and A. M. Abbosh, "Simple design procedure of a broadband circularly polarized slot monopole antenna assisted by characteristic mode analysis,"*IEEE Access*, vol. 6, pp. 78386-78393, 2018.

[24] S. Mohammadi and J. Nourinia, "Compact broadband circularly polarized slot antenna using two linked elliptical slots for C-band applications," *IEEE Antennas Wireless Propag. Lett.,* vol. 12, pp. 1094–1097, 2013.

[25] N. Felegari and J. Nourinia, "Broadband CPW-fed circularly polarized square slot antenna with three inverted-L-shape grounded strips," *IEEE Antennas Wireless Propag. Lett.,* vol. 10, pp. 274–277, 2011.

[26] W. L. Chen, G. M. Wang, and C. X. Zhang, "Bandwidth enhancement of a microstrip-line-fed printed wide-slot antenna with a fractal-shaped slot," *IEEE Trans. Antennas Propag.,* vol. 57, pp. 2176–2179, July 2003.

[27] H. Zhang, Y.-C. Jiao, L. Lu, and C. Zhang, "Broadband circularly polarized square-ring-loaded slot antenna with flat gains,"*IEEE Antennas Wireless Propag. Lett.,*vol. 16, pp. 29–32, 2017.

[28] S. Koziel, and A. Bekasiewicz, "Expedited geometry scaling of compact microwave passives by means of inverse surrogate modeling," *IEEE Trans. Microwave Theory Tech.*, vol. 63, no. 12, pp. 4019-4026, 2015.

[29] U. Ullah and S. Koziel, "A geometrically simple compact wideband circularly polarized antenna," *IEEE Antennas Wireless Propag. Lett.,*vol. 18, no. 6, pp. 1179-1183, June 2019.

[30] S. Koziel, and A. Bekasiewicz, "Inverse surrogate modeling for low-cost geometry scaling of microwave and antenna structures," *Eng. Comp.*, vol. 33, no. 4, pp. 1095-1116, 2016.

[31] S. Koziel, J.W. Bandler, and Q.S. Cheng, "Robust trust-region space-mapping algorithms for microwave design optimization," *IEEE Trans. Microwave Theory and Tech.*, vol. 58, no. 8, pp. 2166-2174, 2010.

[32] A. Pietrenko-Dabrowska and S. Koziel, "Numerically efficient algorithm for compact microwave device optimization with flexible sensitivity updating scheme," *Int. J. RF & Microwave CAE*, 2019.

[33] C.G. Broyden, "A class of methods for solving nonlinear simultaneous equations," *Math. Comp.*, vol. 19, pp. 577-593, 1965.

[34] Y. He, W. He, and H. Wong, "A wideband circularly polarized cross-dipole antenna," *IEEE Antennas and Wireless Propag. Lett.*, vol. 13, pp. 67–70, 2014.

[35] M. Nosrati and N. Tavassolian, "Miniaturized circularly polarized square slot antenna with enhanced axial-ratio bandwidth using an antipodal y-strip," *IEEE Antennas Wireless Propag. Lett.*, vol. 16, pp. 817–820, 2017.

[36] R. K. Saini, S. Dwari, and M. K. Mandal, "CPW-Fed dual-band dual-sense circularly polarized monopole antenna," *IEEE Antennas Wireless Propag. Lett.*, vol. 16, pp. 2497–2500, 2017.

[37] H. G. Xue, X. X. Yang, and Z. Ma, "A novel microstrip-CPW fed planar slot antenna with broadband and circular polarization," *IEEE Antennas Wireless Propag. Lett.*, vol. 14, pp. 1392–1395, 2015.

[38] M. S. Ellis, Z. Zhao, J. Wu, X. Ding, Z. Nie, and Q.H. Liu, "A novel simple and compact microstrip-fed circularly polarized wide slot antenna with wide axial ratio bandwidth for C-band applications," *IEEE Trans. Antennas Propag.*, vol. 64, no. 4, pp. 1552–1555, 2016.

[39] J.Y. Jan, C.Y. Pan, K.Y. Chiu, and H.M Chen, "Broadband CPW-fed circularly-polarized slot antenna with an open slot," *IEEE Trans. Antennas Propag.,* vol.61, no. 3, pp. 1418–1422, 2013.

[40] Y. Ojaroudi, N. Ojaroudi, and N. Ghadimi, "Circularly polarized microstrip slot antenna with a pair of spur-shaped slits for WLAN applications," *Microw. Opt. Technol. Lett.*, vol. 57, pp. 756–759, 2015.

[41] S. Fakhte, H. Oraizi, R. Karimian, and R. Fakhte, "A new wideband circularly polarized stair-shaped dielectric resonator antenna," *IEEE Trans. Antennas Propag.,*vol.63, no. 4, pp. 1828–1832, 2015.

[42] K. O. Gyasi, G. Wen, D. Inserra, Y. Huang, J. Li, A. E. Ampoma , and H. Zhang, "A compact broadband cross-shaped circularly polarized planar monopole antenna with a ground plane extension," *IEEE Antennas Wireless Propag. Lett.*, vol. 17, no. 2, pp. 335–338, 2018.

UBAID ULLAH received the M.Sc and PhD degree in electrical and electronic engineering from the Universiti Sains Malaysia, in 2013 and 2017, respectively. During his PhD, he was awarded the prestigious global fellowship and the outstanding student award. He was with Engineering Optimization & Modeling Center, School of Science and Engineering, Reykjavik University, Iceland from late 2017 to early 2019. He is currently working as a postdoctoral research fellow at the Al Ain University of Science and Technology, Abu Dhabi, UAE. He has published a number of high-quality journal articles and participated in some well-reputed international conferences. His research interest includes antenna theory, small antennas, antenna polarization, dielectric resonators, waveguides, millimeter-wave antenna designs, multiple-input multiple-output (MIMO) antenna system, EM-simulation-driven design, numerical analysis, microwave circuit design, and optimization.

SLAWOMIR KOZIEL received the M.Sc. and Ph.D. degrees in electronic engineering from the Gdansk University of Technology, Poland, in 1995 and 2000, respectively, the M.Sc. degree in theoretical physics and the M.Sc. and Ph.D. degrees in mathematics from the University of Gdansk, Poland, in 2000, 2002, and 2003, respectively. He is currently a Professor with the School of Science and Engineering, Reykjavík University, Iceland. His research interests include CAD and modeling of microwave and antenna structures, simulation-driven design, surrogate-based optimization, space mapping, circuit theory, analog signal processing, evolutionary computation, and numerical analysis.

ISMAIL BEN MABROUK received the B.A.Sc. and M.A.Sc. degrees in electrical engineering from the University of Lille, Lille, France in 2006 and 2007, respectively and the PhD in Electrical Engineering from University of Quebec, Canada, in 2012. From 2007 to 2009 he was with Huawei Technologies, Paris, France. In 2012, he joined the Wireless Devices and Systems (WiDeS) group at University of Southern California, Los Angeles, USA. He is currently an Assistant Professor at Al Ain University of Science and Technology, Abu Dhabi, UAE. His research activities have been centred on propagation studies for Multiple-Input and Multiple-Output (MIMO) systems, measurement campaigns in special environments, WBAN, and antenna design at the millimiter-wave and THz frequencies.